# Uplink NOMA for Heterogeneous NTNs with LEO Satellites and High-Altitude Platform Relays

Matthew Bliss[1], Frederick J. Block[2], Thomas C. Royster[3], and David J. Love[1]
[1]School of Electrical and Computer Engineering, Purdue University, West Lafayette, IN 47906, U.S.A.
[2]MIT Lincoln Laboratory, Lexington, MA 02421, U.S.A.
[3]LinQuest Corporation, Lexington, MA 02421, U.S.A.
Emails: {blissm,djlove}@purdue.edu, {troyster,fblock}@ll.mit.edu

***Abstract*—An uplink non-orthogonal multiple-access communication system is developed for heterogeneous non-terrestrial networks (NTNs) that employ both low-Earth orbit (LEO) satellite constellations and high-altitude platforms (HAPs) as relays with hybrid automatic repeat request capabilities. The system is designed as a random-access and interference-resistant network to support low-rate users. A common waveform and frequency band is used for all uplink transmissions (whether the transmitter is a user terminal or a HAP). Both theoretical and simulation-based performance analysis results are provided as a function of user transmit power and packet arrival rates for channels with interference. The use of HAP relays is shown to significantly improve throughput and reduce queue size relative to direct transmission to the LEO satellites, especially for the case of low-power users in high interference environments.**

## I. Introduction

In the ongoing design of sixth-generation (6G) networks, the projected surge in connected devices will strain conventional terrestrial network infrastructure [1]. However, the emergence of non-terrestrial networks (NTNs) that provide connectivity to under-served, remote areas and substantially boost the connectivity of well-served areas [2] may alleviate this strain. Low-Earth orbit (LEO) satellite communications (Satcom) constellations, in particular, are being designed and fielded to provide enhanced connectivity in the form of the massive proliferation of LEO satellites, e.g., Starlink, OneWeb, and Kuiper [3]–[5].

The emerging LEO Satcom systems place a massive number of satellites into orbit, hence the user equipment (UE) has more than one satellite in its field of view (FOV) with which it can communicate, and the system's scheduling service determines which satellite the terminal is assigned to at each moment. As the major proliferated LEO Satcom constellations support user links at Ku or Ka band [6], the user uplink beams are relatively narrow and high gain, thus providing directionality to the assigned satellite and generally high data rates, respectively.

However, direct ground-to-LEO satellite communication poses challenges such as high Doppler shifts and frequent handovers [7]. NTNs, which include LEO satellites but may also incorporate additional vertical layers such as unmanned aerial vehicles (UAVs) and high altitude platforms (HAPs), provide a unique opportunity for the development of 6G networks to improve connectivity by integrating a hierarchical structure of macro-to-micro cells (coverage regions) that leverage the diversity provided by the vastly different altitudes of the heterogeneous non-terrestrial receivers [8].

We propose a heterogeneous NTN system sharing several similarities with commercially proliferated LEO constellations, except the targeted service is reliable satellite communications for users with small terminals, the UEs, who wish to communicate short messages. The system is designed to support a large number of users, each with a relatively small probability of transmission. This is accomplished with a spread-spectrum waveform that supports non-orthogonal multiple access (NOMA) [9]. The system consists of UEs, a high altitude platform (HAP) relay layer, and the backbone LEO network. To further improve resiliency, each LEO satellite may include a receive sparse antenna array that enables spatial discrimination over its FOV.

In this paper, we study the uplink scenario for the UEs. Using the HAP to relay messages to the LEO backbone provides several benefits to a low-power UE. The UE-to-HAP link has a shorter distance than the UE-to-LEO link (hence lower path loss) and may allow improved elevation angles which reduces blockage [10]. Additionally, as the second-hop transmitter, the HAP may be able to utilize higher transmit power and increased antenna gain relative to a UE when attempting to close the longer link to a LEO satellite. By relaying UE uplink packets through a stationary HAP, a large group of packets appear to the LEO satellite as originating from a single location, which can reduce computational demands on resource management processes such as handovers as well as Doppler compensation. HAPs also generally have a smaller FOV than satellites, which provides passive discrimination against interferers [10].

In the heterogeneous NTN relaying system proposed in this paper, the users, e.g., agricultural sensors and low-power wide-area network (LPWAN) devices [11], utilize wide transmit and receive beams, so that they do not have to actively point at specific receivers. Services designed in the Ultra High Frequency (UHF) band, such as Narrowband Internet of Things (NB-IoT) applications [12], are examples of applications that can benefit

DISTRIBUTION STATEMENT A. Approved for public release. Distribution is unlimited. This material is based upon work supported by the Department of the Air Force under Air Force Contract No. FA8702-15-D-0001. Any opinions, findings, conclusions or recommendations expressed in this material are those of the author(s) and do not necessarily reflect the views of the Department of the Air Force.

from our proposed system. The wide transmit and receive beams provide flexibility in the composition and operation of the relay layer.

The distinct advantages offered by the HAP relay layer will be shown to drastically increase UE throughput in numerical simulations when compared to direct UE-LEO uplink transmission. Most importantly, it is shown that low-power UEs in high interference environments especially benefit from the additional HAP relay layer. In our paper, the HAPs receive user transmissions and forward them to the Satcom layer. Several specific implementation options for this role are possible, including error correction prior to next-hop transmission, e.g., decode-and-forward (DF), or simplify amplification of user terminal signals, e.g., amplify-and-forward (AF). In our model, the HAP decodes data after receiving the entire frame from a UE, i.e., DF protocols are used. The role of feedback is considered, and Chase combining hybrid automatic repeat request (HARQ) [13] is employed as a retransmission scheme on both the UE-HAP and HAP-LEO links.

## II. System Model

In this section, we develop the system model, beginning with an overview of the network topology, the multiple access protocol (including the retransmission scheme), the link budget and signal-to-interference-plus-noise-ratio (SINR) calculations, and a description of the forward error correction (FEC) coding scheme and its associated decoding error probability calculation.

### A. Network Overview

A straightforward model is used to analyze the effectiveness of a HAP relay for facilitating uplink UE-LEO communication. As depicted in Fig. 1, we consider one HAP at the origin (on the $x$-$y$ ground plane) and elevated to the fixed height $h_H$ km and one LEO at the origin and elevated to the fixed height $h_L$ km, where $h_H < h_L$. The HAP and LEO have circular coverage areas on the ground plane, both centered at the origin, with radii $a_H$ km and $a_L$ km, respectively, where $a_H < a_L$. All uplink UEs are located on the ground plane and inside the HAP coverage area (and consequently the LEO coverage area).

Inside the HAP coverage area, there are $N_U$ UEs, with each user position selected independently according to a uniform circular distribution; additionally, every UE utilizes power control. In addition to the UEs, $N_I$ other higher-powered users communicating directly to LEO satellites are modeled as interferers and are uniformly distributed throughout the encompassing LEO coverage region; each interferer uses the same transmission power. Power control is not assumed for the higher-powered interferers, as they are communicating directly with LEO satellites within their FOV (which may not be the same satellites). From time slot to time slot, the interferer locations are independent and identically distributed (i.i.d.) following the uniform circular distribution. Finally, both the UEs and interferers utilize direct sequence spread spectrum (DS-SS) with spreading factor $W$ and carrier frequency $f_c$.

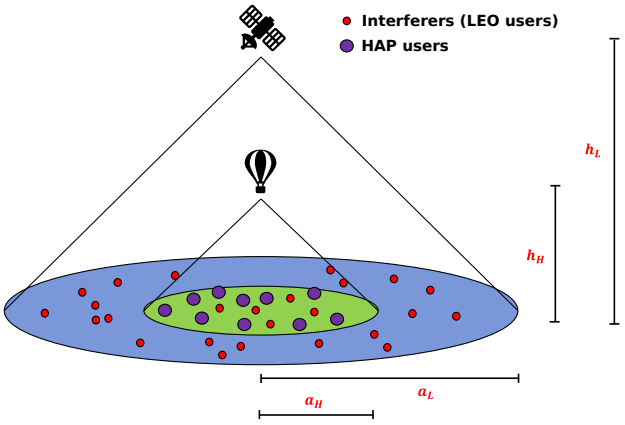


Fig. 1. System model.

### B. Multiple Access Protocol

The uplink employs a slotted random access MAC layer. A user transmission in a slot is called a frame; each frame consists of an acquisition header and a data payload. Frames employ spread spectrum modulation, providing robustness against interference. The same waveform and spectrum is used regardless of the destination type. This approach is consistent with the overall system vision of the relay layer being a collection of sensors, each independently attempting to recover as many uplink transmissions from terminals as possible.

Each UE independently generates a frame during a slot with probability $p_a$. Newly generated frames are added to the user's queue while ongoing transmissions or retransmissions occur. Once the UE frame is ready to transmit, transmission occurs in the next available time slot. We assume that error-free feedback is provided to users acknowledging the success of frame reception at the HAP (for payloads transmitted by the UEs) and at the LEO (for payloads transmitted by the HAP) before the next time slot. In fact, the downlink control channel used to send acknowledgments is not modeled explicitly but is assumed to provide high reliability and operates on separate spectrum resources.

If the UE does not receive an acknowledgment of successful receipt, it retransmits the frame in the next time slot with probability $p_{r,U}$. The HAP transmits successfully decoded received frames to the LEO in the subsequent time slot. Additionally, the HAP retransmits unacknowledged frames transmitted to the LEO in the subsequent time slot with probability $p_{r,H}$. Moreover, the probability that an interferer is active in a time slot occurs with probability $p_I$, i.i.d. for all $N_I$ higher-powered interferers.

To further augment the performance gains provided by using a HAP relay, decoding failures at the HAP and LEO (i.e., the UE-HAP and HAP-LEO links), utilize Chase combining automatic repeat request (HARQ) [13]. Essentially, the receiver of interest stores the received values of past frame transmission attempts and uses the signal data from the original transmission and all retransmissions to improve the effective SINR used for decoding the data payload. The

effective receive SINR on a linear scale is recombined as

$$SINR_{\text{tot}} = SINR_0 + SINR_{\text{rtx},1} + \ldots SINR_{\text{rtx},N}, \quad (1)$$

where the subscript 0 indicates the original frame transmission, and $(\text{rtx}, i)$ is the $i$-th retransmission. In this model, the SINR value of a reception is assumed to be the average SINR across the entire data frame, and it is assumed that bit-wise errors occur with equal probability across the frame, i.e., the noise power is distributed equally over the bits within the same time slot. In the next subsection, we discuss the link budget calculation and associated derivation of the SINR.

### C. Receiver Models and Link Budgets

The received power of each UE signal at the HAP is identical in a given time slot due to the power control protocol. A UE located on the ground plane and at the origin, directly below the HAP a distance $h_H$ km away, is used as a reference point. The reference transmit power, denoted by $P_{\text{tx},U}$ (in dBW), for this UE is then used to calculate the transmit power required for all UEs in the HAP coverage area to yield the same received power at the HAP. All UEs have omni-directional antennas (no transmit antenna gain). The HAP has a constant receive antenna gain throughout its entire coverage area, given by $G_{\text{rx},H}$ dBW. The per-user received power at the HAP is calculated as

$$P_{\text{rx},H} = P_{\text{tx},U} + G_{\text{rx},H} - PL(h_H, f_c), \quad (2)$$

where $PL(\cdot,\cdot)$ is the free space path loss, dependent on the reference distance $h_H$ and carrier frequency $f_c$.

The HAP transmits to the LEO using a fixed total transmit power $P_{\text{tot},H}$. As the HAP is resource-limited, the total available power is equally divided by all active UE frames transmitting or retransmitting through the HAP in a time slot. The per-user effective isotropic radiated power (PEIRP) is thus dependent on the total number of active HAP frame transmissions in a slot, which depends on the UE-HAP link total throughput, the throughput of the HAP-LEO link, and the HAP retransmission probability $p_{r,H}$.

The HAP uses a transmit antenna with a constant gain $G_{\text{tx},H}$ dBW. At the LEO receiver, a sparse array with constant gain $G_{\text{rx},L}$ dBW is seen by frames transmitted by the HAP, as it is assumed that beamforming provides a constant gain to the stationary HAP. For the interference sources and ground-based UEs also transmitting during the frame, however, a random gain is seen in each time slot, in line with the behavior of the large sparse array and the random realizations of UE and interferer locations from one time slot to the next. The per-user received power at the LEO in the $i$-th time slot is thus given (in dBW) as

$$P_{\text{rx},L}(i) = \frac{P_{\text{tot},H}}{M_i} + G_{\text{tx},H} + G_{\text{rx},L} - PL(h_L - h_H, f_c), \quad (3)$$

where $M_i$ is the total number of frames being transmitted by the HAP in time slot $i$, including both newly decoded received frames and possible retransmissions from prior time slots.

At the HAP, the receive SINR of an individual frame received in time slot $i$ is described by

$$\Gamma_{\text{rx},H}(i) = \frac{P_{\text{rx},H}}{N + \frac{1}{W}(N_i - 1) P_{\text{rx},H} + \frac{1}{W} P_{\text{int},H}}, \quad (4)$$

where $N$ is the total noise power, $W$ is the DS-SS spreading factor, $N_i$ is the number of active UEs in time slot $i$, and $P_{\text{int},H}$ is the total power received from all non-UE interferers; in fact, $P_{\text{int},H}$ is a function of the number of active interferers in a time slot (random variable determined by the probability $p_I$), the uniform circular distribution of interferers in the LEO coverage area (also a random realization in each time slot), and the transmit power of the interferers. From slot to slot, the interference contribution is necessarily a random variable. For $\Gamma_{\text{rx},H}(i)$ in equation (4), we neglect HAP transmissions as a source of interference for frame receptions at the HAP, as it is assumed that the HAP is a sizable physical body, the receive and transmit antenna structures are on the bottom and top of the HAP, respectively, and the main lobe of the HAP transmit antenna faces upward toward the LEO satellite.

Similarly, at the LEO satellite, the receive SINR of an individual frame received in time slot $i$ is given by

$$\Gamma_{\text{rx},L}(i) = \frac{P_{\text{rx},L}(i)}{N + \frac{1}{W}\left[(M_i - 1) P_{\text{rx},L}(i) + P_{\text{int},U} + P_{\text{int},L}\right]}, \quad (5)$$

where $P_{\text{int},L}$ is the total ground-based interference power coming from non-HAP users dispersed in the LEO coverage area; it is a random realization of the active interferer locations, as well as a random LEO receive antenna gain, as determined by the sparse array to be described. Moreover, $P_{\text{int},U}$ is the total interference experienced at the LEO due to UEs transmitting to the HAP in time slot $i$; it is determined by the arrival rate, UE-HAP link throughput, retransmission probability, and a random LEO receive antenna gain applied to each user, due to the time-varying locations of the UEs throughout the HAP coverage area.

Finally, we formalize the LEO receive antenna structure and the associated random gain as seen by both interferers and HAP users. As opposed to the HAP, the LEO's high elevation, large FOV, and increased technological complexity permit it to be outfitted with a large sparse array, providing a large coverage area in which both LEO users (modeled as interference) and HAP users are encapsulated. The LEO received antenna gain distribution (as seen by the interferers and ground-based HAP users) is modeled, in linear units, as an exponential distribution with mean $1/\mu$. Due to the wide LEO coverage area and the fact that beamforming focuses the main lobe in the direction of the HAP, most positions in the coverage area will not be in view of the main lobe. Due to the size of the sparse array and the large geographical dispersion of transmitters on the ground, we invoke the statistical argument that the in-phase and quadrature components of transmitted signals receive random, zero-mean Gaussian signal distortions, which coincide with the exponential distribution of the antenna gain, i.e., the square of the magnitude of a complex Gaussian is exponential [14]. In each time slot, each interferer and HAP

user that interferers at the LEO receiver is designated a gain drawn i.i.d. randomly from an exponential distribution with mean $1/\mu$ (which can be converted into dB units as well).

### D. Forward Error Correction Decoding Error

In this paper, we model each frame as a codeword of a linear code, with each frame encoded using a $(648, 432)$ binary low-density parity check (LDPC) code with rate $2/3$, used and described in [13]. This coding scheme is used due to 1) its performance capabilities, and 2) the availability of a well-fitted codeword error probability as a function of the per-bit SINR. The packet error rate (PER) function for this code is explained in [13]; however, it is hard to write and based on the complementary Gaussian $Q$-function. To provide analytical intuition for the PER, and for easy numerical implementation, we fit the PER with a reverse sigmoid function, given as

$$\mathrm{PER}(x) = \frac{e^{-7.2(x-1.03)}}{e^{-7.2(x-1.03)} + e^{7.2(x-1.03)}}, \tag{6}$$

where $x = \Gamma/D$, where $\Gamma$ is the SINR (in linear units) and $D$ is the data rate.

## III. Theoretical Analysis

In this section, we perform a two-fold theoretical analysis. First, we derive closed-form approximations for the receive SINR for frames received at both the HAP and LEO. With the approximations in place, we develop a steady-state Markov chain analysis of the UE-HAP link throughput that verifies simulation results shown in Sec. IV, in addition to providing an analytical model for future use in studying HARQ-enabled HAP relaying systems. In future work, attention will also be given to the HAP-LEO link and the end-to-end throughput of this relaying system.

### A. Analytical SINR Calculations

As a key component of the analysis, we assume that due to the close proximity of the HAP to its users, compared to other interferers assumed to be communicating with LEO satellites, the interferers use much higher transmit power and dominate the total interference. In other words, the multiple-access interference due to the HAP users (i.e., the UEs) is treated as negligible for frames received at both the HAP and the LEO. Since the LEO coverage area is wide, the number of possible interferers in the region is expected to be on the order of hundreds or thousands. For this case, we approximate the frame SINR in a given time slot as its *expected value*.

For the UE-HAP link, we let $P_{\mathrm{tx,int}}$ be the individual transmit power of each interferer. Assuming the interferers also use omni-directional antennas, the closed-form approximation to the total power received from all non-UE interferers, $P_{\mathrm{int},H}$ (in W), is given by

$$\begin{aligned} P_{\mathrm{int},H} &= \int_0^{a_H} \frac{P_{\mathrm{tot},I} \cdot g_{\mathrm{rx},H} \cdot \beta_0}{h_H^2 + r^2} \cdot \frac{2r}{a_H^2} \mathrm{d}r \\ &= \frac{P_{\mathrm{tot},I} \cdot g_{\mathrm{rx},H} \cdot \beta_0}{a_H^2} \log\left(\frac{a_H^2 + h_H^2}{h_H^2}\right), \end{aligned} \tag{7}$$

where $P_{\mathrm{tot},I} \triangleq N_I \cdot p_I \cdot P_{\mathrm{tx,int}}$ is the expected total transmit power of all interferers in a time slot, $g_{\mathrm{rx},H} = 10^{G_{\mathrm{rx},H}/10}$ is the HAP receive antenna gain (in linear units), $\beta_0$ is the carrier frequency-dependent path loss proportionality factor, $a_H$ and $h_H$ are the previously mentioned HAP coverage radius and elevation, respectively. The presence of the natural logarithm factor comes from taking the expectation of the interferer locations according to the radial component (on the ground-plane) of the uniform circular distribution, $f_R(r) = (2r)/a_H^2$ with $r \in [0, a_H]$.

For the HAP-LEO link, we similarly derive a closed-form expression for the power $P_{\mathrm{int},L}$ (in W) as

$$\begin{aligned} P_{\mathrm{int},L} &= \int_0^{a_L} \frac{P_{\mathrm{tot},I} \cdot \beta_0}{\mu\left(h_L^2 + r^2\right)} \cdot \frac{2r}{a_L^2} \mathrm{d}r \\ &= \frac{P_{\mathrm{tot},I} \cdot \beta_0}{\mu a_L^2} \log\left(\frac{a_L^2 + h_L^2}{h_L^2}\right), \end{aligned} \tag{8}$$

where $a_L$ and $h_L$ are the previously mentioned LEO coverage radius and elevation, respectively, $1/\mu$ is the expected receive antenna gain (in linear units) of the sparse array at the LEO, and the radial component of the uniform circular distribution used is $f_R(r) = (2r)/a_L^2$ with $r \in [0, a_L]$.

Substituting the approximations (7) and (8) into the SINR calculation and dropping the multiple-access interference contribution from other UEs, we obtain SINR approximations for received frames at the HAP and LEO, respectively, as

$$\tilde{\Gamma}_{\mathrm{rx},H} = \frac{P_{\mathrm{rx},H}}{N + \frac{1}{W} P_{\mathrm{int},H}}, \tag{9}$$

$$\tilde{\Gamma}_{\mathrm{rx},L} = \frac{P_{\mathrm{rx},L}(i)}{N + \frac{1}{W}\left[\left(M_i - 1\right) P_{\mathrm{rx},L}(i) + P_{\mathrm{int},L}\right]}, \tag{10}$$

noting that (9) is a constant value, and (10) varies depending on the number of frames being transmitted by the HAP in time slot $i$ (due to the total HAP transmit power getting divided equally among the total number of frames).

### B. Markov Chain Analysis of UE-HAP Throughput

Next, we apply the SINR approximation (9) (a constant value for this case) and derive a Markov chain model to be used to theoretically calculate the throughput for the UE-HAP link. To make the model tractable, we assume that 1) all UEs are operating in the saturated queue mode, meaning once a frame is successfully acknowledged by the UE, a new packet is transmitted in the next time slot; and 2) we enforce a maximum allowable number of retransmissions so that the Markov chain has a finite number of states, with the maximum number of retransmissions chosen so that the PER is vanishingly small (5-6 retransmissions in our simulations).

As a consequence of the constant frame SINR approximation, subsequent retransmissions of failed frame decodings recombine using Chase combining HARQ at the HAP so that the effective SINR after the original transmission and $j$ retransmissions is $(j+1)\tilde{\Gamma}_{\mathrm{rx},H}$. Letting the data-rate-normalized SINR be $x = \tilde{\Gamma}_{\mathrm{rx},H}/D$, the probability of correct decoding on the $j$-th retransmission is thus given by

$$\sigma_{jx} = \mathrm{PER}\left(\left(j+1\right)x\right), \tag{11}$$

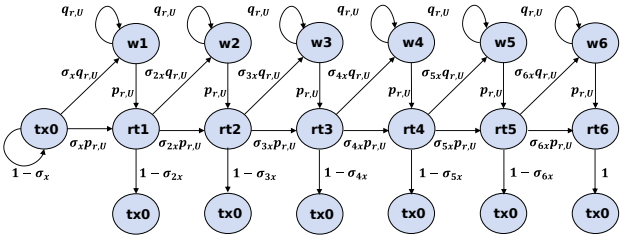


Fig. 2. Markov chain state transition diagram.

TABLE I
TRANSMISSION POWER, COVERAGE RADII, AND ANTENNA GAINS

| | | |
|---|---|---|
| Reference UE Tx power | 0.01-5.0 | W |
| HAP total Tx power | 10-25 | W |
| Interferer Tx power | $> 10\times$ [Variable] | W |
| HAP coverage radius | 50 | km |
| LEO coverage radius | 2000 | km |
| HAP Tx antenna gain | 2.4 | dBW |
| LEO mean Rx antenna gain | 8.3 | dBW |
| No. HAP interferers | 150 | interferers |
| No. LEO interferers | 2000 | interferers |
| No. network users | 150 | users |
| Data rate | 6.48 | kbps |
| DS-SS spreading | 20 | MHz |
| Carrier frequency | 300 | MHz |
| Packet arrival prob. | $(0, 1)$ [Variable] | per slot |
| Re-Tx prob. | $(0, 1)$ [Variable] | per slot |

where $\mathrm{PER}(\cdot)$ is given in (6). For the saturated queue, the packet arrival probability is set to $p_a = 1$; we denote the complement of the retransmission probability $p_{r,U}$ with $q_{r,U} = 1 - p_{r,U}$. The original transmission state of the Markov chain is given by $\mathrm{tx}$, the states waiting to retransmit are $\mathrm{w}$, and the retransmission attempt states are $\mathrm{rt}$. Using this notation, the Markov chain is depicted in Fig. 2 with the maximum number of retransmissions set to $M_{\mathrm{rtx,max}} = 6$. The analytical throughput of the UE-HAP link can be calculated by filling out the state transition probability matrix, self-multiplying the matrix sufficiently many times so that the columns converge to the steady-state. The normalized per-user throughput can be obtained using the steady-state probabilities and can be readily converted into the aggregate throughput calculation.

## IV. Numerical Results

In this section, we perform numerical simulations to demonstrate the efficacy of the UE-HAP-LEO relaying system. For all simulations, the LEO and HAP altitudes are fixed at $h_L = 800$ km and $h_H = 20$ km, respectively. The transmission powers, coverage radii, and antenna gains are displayed in Table I, as well as the number of interferers seen by the HAP and LEO, number of network users, data rate, signal spreading factor, packet arrival, and retransmission rate.

To demonstrate the performance gains provided by the HARQ-enabled HAP relay, Fig. 3 shows the uplink throughput for the UE-HAP and HAP-LEO links compared to direct UE-LEO transmission. For each subfigure, the total HAP transmit power is fixed to 20W. In each subplot, the UE reference transmit power is fixed at 0.1W, and the power per-interferer is varied between 1-12W. The UE and HAP retransmission

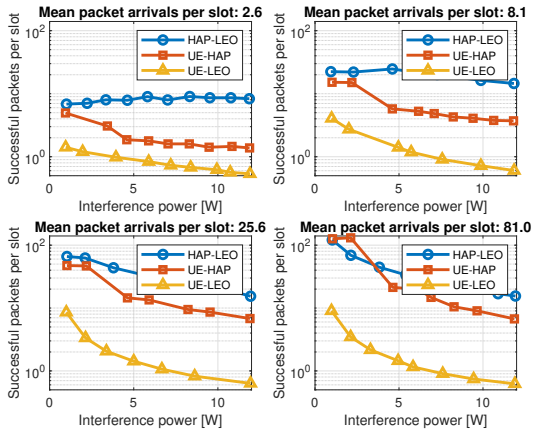


Fig. 3. Throughput vs. interference power for various aggregate traffic intensities.

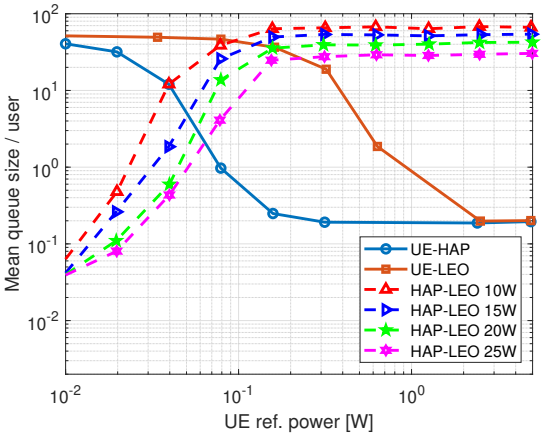


Fig. 4. Per-user mean queue size vs. UE reference transmit power for various communication links.

probabilities are both set to $0.25$. Each subplot is for a distinct aggregate mean packet arrival per time slot, and the throughput is measured as the average number of successfully decoded packets per slot. For each subplot, throughput on the relaying links is consistently above that of direct UE-LEO transmission. The HAP-LEO throughput generally dominates that of the UE-HAP link. Thus in the uplink setting, the second hop is not a bottleneck and operates in a feasible region, i.e., the queue at the HAP is much less likely to have extremely large values.

Most important is the observation that the HARQ-enabled HAP relay provides two-fold gains: as the first-hop receiver, the shorter propagation distance to the UEs reduces pathloss, improving the SINR and the probability of correct packet decoding; as the second-hop transmitter, the HAP simultaneously reduces propagation distance to the LEO and provides some upward antenna directionality compared to the simple isotropic UE antennas. This combination drastically improves the relay throughput when compared to direct UE-LEO transmission (using the same HARQ protocol for fair comparison).

In Fig. 4, the mean per-user queue size (each user has its own queue at the HAP) is shown as the UE reference transmit

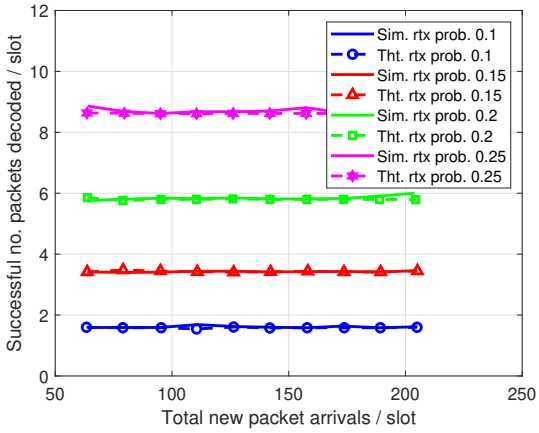


Fig. 5. Total throughput of UE-HAP link vs. aggregate traffic intensity for simulations and theoretical Markov chain analysis.

power varies between 0.01-5W. The per-interferer transmit power is fixed at 5W. The mean queue size is shown for the UE-HAP link and HAP-LEO links for multiple total HAP powers, as well as direct UE-LEO transmission. As the UE reference power increases, the queues at the UEs decrease for both the first hop (UE-HAP link) and direct transmission, with the queues being lower for the UE-HAP link due to the improved channel quality and shorter propagation distance to the HAP. However, as the UE reference power increases, more packets are successfully decoded at the relay, and the queue size of the HAP-LEO link increases, as the total available transmit power at the HAP is divided among a larger number of successful packets in each time slot. The use case most benefited by the HAP relay is the low-to-moderate power regime with high interference (see the range of 0.05-0.08W UE reference power compared to 5W per interferer). Here, the mean UE queue size is well below that of direct transmission; provided the HAP has ample total transmit power (e.g., 20-25W), the queue size of the second hop also remains low.

In Fig. 5, the aggregate throughput per time slot is shown for various levels of data traffic intensity. In this figure, we compare the simulation results to the Markov chain analysis on the UE-HAP link for the saturated queue case. We vary the retransmission probability over several values. For this simulation, the UE reference transmit power is fixed to 0.1W; the interferer transmit power is fixed to 5W; and the packet arrival probability is $p_a = 1$ (saturated queue). From Fig. 5, it is clear that given a retransmission probability, the throughput of the theoretical simulation and Markov chain analysis align very closely for the case of the saturated queue. In fact, over the various retransmission probabilities tested, the simulation throughput is consistently within 4% of the Markov chain analysis for all except one testing point.

## V. Conclusion

In this paper, we developed a HAP-assisted satellite relaying system employing error correction and HARQ protocols for uplink data transmission. It was shown that the HAP relay greatly improves throughput and queue size performance compared to direct user-satellite transmission, especially for the case of low-power users sharing waveform and spectrum resources in a high interference environment. Simulations are verified by a Markov chain analysis to be used in future research of HARQ-enabled heterogeneous NTN systems.

## References


[1] G. Hernandez, "From People to Things: Building Global Connectivity," *Organisation for Economic Cooperation and Development. The OECD Observer*, p. 1J, 2017.

[2] N. Saeed, H. Almorad, H. Dahrouj, T. Y. Al-Naffouri, J. S. Shamma, and M.-S. Alouini, "Point-to-Point Communication in Integrated Satellite-Aerial 6G Networks: State-of-the-Art and Future Challenges," *IEEE Open Journal of the Communications Society*, vol. 2, pp. 1505–1525, 2021, doi: 10.1109/OJCOMS.2021.3093110.

[3] O. Kodheli *et al.*, "Satellite Communications in the New Space Era: A Survey and Future Challenges," *IEEE Communications Surveys & Tutorials*, vol. 23, no. 1, pp. 70–109, Firstquarter 2021, doi: 10.1109/COMST.2020.3028247.

[4] B. Di, L. Song, Y. Li, and H. V. Poor, "Ultra-Dense LEO: Integration of Satellite Access Networks into 5G and Beyond," *IEEE Wireless Communications*, vol. 26, no. 2, pp. 62–69, April 2019, doi: 10.1109/MWC.2019.1800301.

[5] I. Leyva-Mayorga *et al.*, "LEO Small-Satellite Constellations for 5G and Beyond-5G Communications," *IEEE Access*, vol. 8, pp. 184 955–184 964, 2020, doi: 10.1109/ACCESS.2020.3029620.

[6] N. Pachler, I. del Portillo, E. F. Crawley, and B. G. Cameron, "An Updated Comparison of Four Low Earth Orbit Satellite Constellation Systems to Provide Global Broadband," *2021 IEEE International Conference on Communications Workshops (ICC Workshops)*, pp. 1–7, 2021, doi: 10.1109/ICCWorkshops50388.2021.9473799.

[7] Y. Su, Y. Liu, Y. Zhou, J. Yuan, H. Cao, and J. Shi, "Broadband LEO Satellite Communications: Architectures and Key Technologies," *IEEE Wireless Communications*, vol. 26, no. 2, pp. 55–61, April 2019, doi: 10.1109/MWC.2019.1800299.

[8] M. Giordani and M. Zorzi, "Non-Terrestrial Networks in the 6G Era: Challenges and Opportunities," *IEEE Network*, vol. 35, no. 2, pp. 244–251, March/April 2021, doi: 10.1109/MNET.011.2000493.

[9] N. Abramson, "Multiple Access in Wireless Digital Networks," *Proc. of the IEEE*, vol. 82, no. 9, pp. 1360–1370, Sep. 1994.

[10] M. S. Alam, G. K. Kurt, H. Yanikomeroglu, P. Zhu, and N. D. Dao, "High Altitude Platform Station Based Super Macro Base Station Constellations," *IEEE Communications Magazine*, vol. 59, no. 1, pp. 103–109, January 2021, doi: 10.1109/MCOM.001.2000542.

[11] Z. Qu, G. Zhang, H. Cao, and J. Xie, "LEO Satellite Constellation for Internet of Things," *IEEE Access*, vol. 5, pp. 18 391–18 401, 2017, doi: 10.1109/ACCESS.2017.2735988.

[12] E. M. Migabo, K. D. Djouani, and A. M. Kurien, "The Narrowband Internet of Things (NB-IoT) Resources Management Performance State of Art, Challenges, and Opportunities," *IEEE Access*, vol. 8, pp. 97 658–97 675, 2020, doi: 10.1109/ACCESS.2020.2995938.

[13] M. Zhang, A. Castillo, and B. Peleato, "Optimizing HARQ and Relay Strategies in Limited Feedback Communication Systems," *Applied Sciences*, vol. 10, no. 21, p. 7917, 2020.

[14] D. Tse and P. Viswanath, *Fundamentals of Wireless Communication*. Cambridge University Press, 2005.